

Modification of the Structure and Nano-Mechanical Properties of LiF Crystals Under Irradiation with Swift Heavy Ions

Jānis MANIKS^{1*}, Ilze MANIKA¹, Roberts ZABELS¹, Rolands GRANTS¹, Kurt SCHWARTZ², Michael SOROKIN³

¹ ISSP, University of Latvia, 8 Kengaraga Str., LV 1063, Riga, Latvia

² GSI, Darmstadt, Planckstrasse 1, D-64219 Darmstadt, Germany

³ Russian Research Centre "Kurchatov Institute", Moscow, Russia

crossref <http://dx.doi.org/10.5755/j01.ms.17.3.583>

Received 01 October 2010; accepted 02 July 2011

The modifications of the structure and hardness of LiF crystals under high-fluence irradiation with MeV- and GeV-energy Au ions have been studied using nanoindentation and atomic force microscopy. The formation of ion-induced dislocations and bulk nanostructures consisting of grains with nanoscale dimensions (50 nm–100 nm) has been observed. The structural modifications are accompanied by a strong ion-induced hardening which is related to dislocation impeding by assemblies of defect aggregates, dislocation loops of vacancy and interstitial types and grain boundaries. For MeV ions, the modifications are localized in a thin surface layer (few μm) where much higher density of deposited energy is reached and deeper stage of aggregation of radiation defects is achieved than for GeV ions with the same absorbed energy.

Keywords: LiF crystals, MeV-energy ions, nanostructuring, nanoindentation, hardening.

1. INTRODUCTION

The modifications of the structure of materials on the micro- and nanometer scale and an improvement of their optical, electrical, mechanical and other properties by the irradiation with beams of swift heavy ions are of importance from both the fundamental and technological standpoint. During the recent decades the attention was focused mainly on damage processes induced by swift heavy ions in the GeV-energy range [1–5]. The GeV- ion-induced effects have been investigated in all classes of materials, ranging from metals, semiconductors and insulators to living cells. A large number of studies have been made on LiF, which is widely used as a model material exhibiting high sensitivity to irradiation and high stability of radiation defects at room temperature. Besides, LiF is a material of technological importance in the areas of dosimeter and optical devices.

The main peculiarity of interaction of GeV-energy ions with dielectrics, such as LiF is the localization of damage in ion tracks [2, 5]. At low or moderate fluences the irradiation typically leads to the formation of far-standing tracks embedded in LiF matrix. At high fluences tracks overlap that leads to the formation of additional defect aggregates via the saturation and coagulation of single defects. At this stage the structural damage leads to the strong increase of structure-sensitive mechanical properties, such as indentation hardness [6–10].

Irradiation of LiF with ions in the MeV-energy range, which deposit a significant fraction of their energy via elastic collisions with the target atoms (nuclear energy loss), shows some peculiarities relative to GeV ions [11–13]. Having a projected range of few micrometers, the MeV ions induce more than one order of a magnitude

higher volume concentration of colour centres than the GeV-energy ions with the same absorbed energy. The high volume concentration of primary Frenkel pairs, on the one hand, leads to a high electron-hole centre recombination, and, on the other hand, to more efficient coagulation processes leading to the formation of F_n -centres as well as halogen molecules (X_2) and their aggregates. These processes strongly depend on the fluence and flux (beam current density). For MeV ions, the modifications are localized within a thin surface layer, where a much higher density of the deposited energy is reached and a deeper stage of aggregation of radiation defects is achieved. It is of interest to compare effects induced by MeV and GeV ions. In the present work modifications of the structure and nano-mechanical properties of LiF crystals under irradiation with MeV- and GeV-energy Au ions are studied using nanoindentation, AFM and chemical etching techniques.

2. EXPERIMENTAL

Experiments were performed on nominally pure LiF single crystals (Korth Kristalle, Germany). Main trace impurities were Mg and Na with the concentration of 20 ppm. The density of dislocations in the non-irradiated samples was about 10^5 cm^{-2} . Samples of $10 \times 5 \text{ mm}^2$ with the thickness between 0.5 mm and 1 mm were cleaved from a crystal block along the (100) planes. The crystals were irradiated at the Tandatron accelerator in Porto Alegre (Brasil) with 3-, 5-, 10-, 12-, and 15-MeV Au ions at fluences of $(10^{12} - 2 \times 10^{14}) \text{ ions/cm}^2$ and ion beam current densities I_{beam} from 6.2 nA/cm^2 to 150 nA/cm^2 . The flux (φ) can be estimated as:

$$\varphi [\text{ions cm}^{-2} \text{ s}^{-1}] = 6.24 \times 10^9 \times i_{beam} / q, \quad (1)$$

where q is the charge of the ion. In order to compare effects induced by MeV and GeV ion irradiations, LiF samples were irradiated at the UNILAC linear accelerator

*Corresponding author Tel.: +371-67-261132; fax: +371-67-132778.
E-mail address: manik@latnet.lv (J. Maniks)

of the GSI, Darmstadt with 2187-MeV Au ions at a fluences of $2 \times 10^{11} - 10^{12}$ ions/cm² with a flux of $\sim 10^8$ ions cm⁻² s⁻¹. All irradiations were performed at room temperature and under normal incidence of the ions to the (100) cleavage face of the crystals. The range and energy loss of incident Au ions of different energy in LiF were calculated using SRIM 2010 [14] (Table 1).

Table 1. Energy, range, electronic energy losses and density of deposited energy of Au ions in LiF

E_{ion} , MeV	Ion range R , μm	Electronic energy losses, % of E_{ion}	Density of deposited energy (E_{ion}/R), MeV/ μm
3	0.67	66.4	4.47
5	1.14	72.1	4.39
10	2.29	79.1	4.37
12	2.75	81.0	4.36
15	3.49	82.9	4.30
2187	92	99	23.7

Characterization of the surface morphology and the structure of the irradiated layer were performed using AFM (Veeco, CPII), optical microscopy and chemical etching techniques. In order to reveal ion-induced structural defects, the FeCl₃ solution as a suitable etchant was used.

Nanoindentation tests were performed by MTS G200 nanoindenter with a Berkovich diamond tip (curvature < 20 nm) using the basic and continuous stiffness measurement techniques. The measurements were conducted at the load resolution < 50 nN, displacement resolution ≥ 1 nm, strain rate 0.05 s^{-1} and harmonic frequency 45 Hz. The nanoindenter was calibrated using a reference sample of fused silica. The hardness, Young's modulus and standard deviation of the measurements were calculated from the experimentally obtained loading-unloading curves by the MTS TestWorks 4 software. The results were averaged from 10 individual measurements. The indentation tests were conducted in ambient air at room temperature.

3. RESULTS

3.1. Evolution of the structure of LiF crystals under irradiation with MeV and GeV Au ions

The evolution of structure of LiF crystals irradiated with 3- and 15-MeV Au ions is shown in Fig. 1, a–d. The irradiation with fluences ($10^{12} - 10^{13}$) ions/cm² results in formation of a large amount of ion-induced dislocations (Fig. 1, a–b). Compared with grown-in dislocations, the size of etch pits of ion-induced dislocations was smaller. The density of dislocations increased with the fluence and reached up to $5 \times 10^9 \text{ cm}^{-2}$ that strongly exceeds the density of dislocations in virgin crystals ($\sim 10^5 \text{ cm}^{-2}$).

After irradiation with ($5 \times 10^{13} - 10^{14}$) ions/cm² the irradiated layer becomes uniformly nanostructured. The AFM images from the cross-section of irradiated crystal prepared by cleaving along the ion pass show a structure consisting of columnar LiF grains with the size of 100 nm–150 nm (Fig. 1, c and d). The thickness of the

nanostructured layer (Fig. 1, c) coincides with the range of 15-MeV ions given in Table 1.

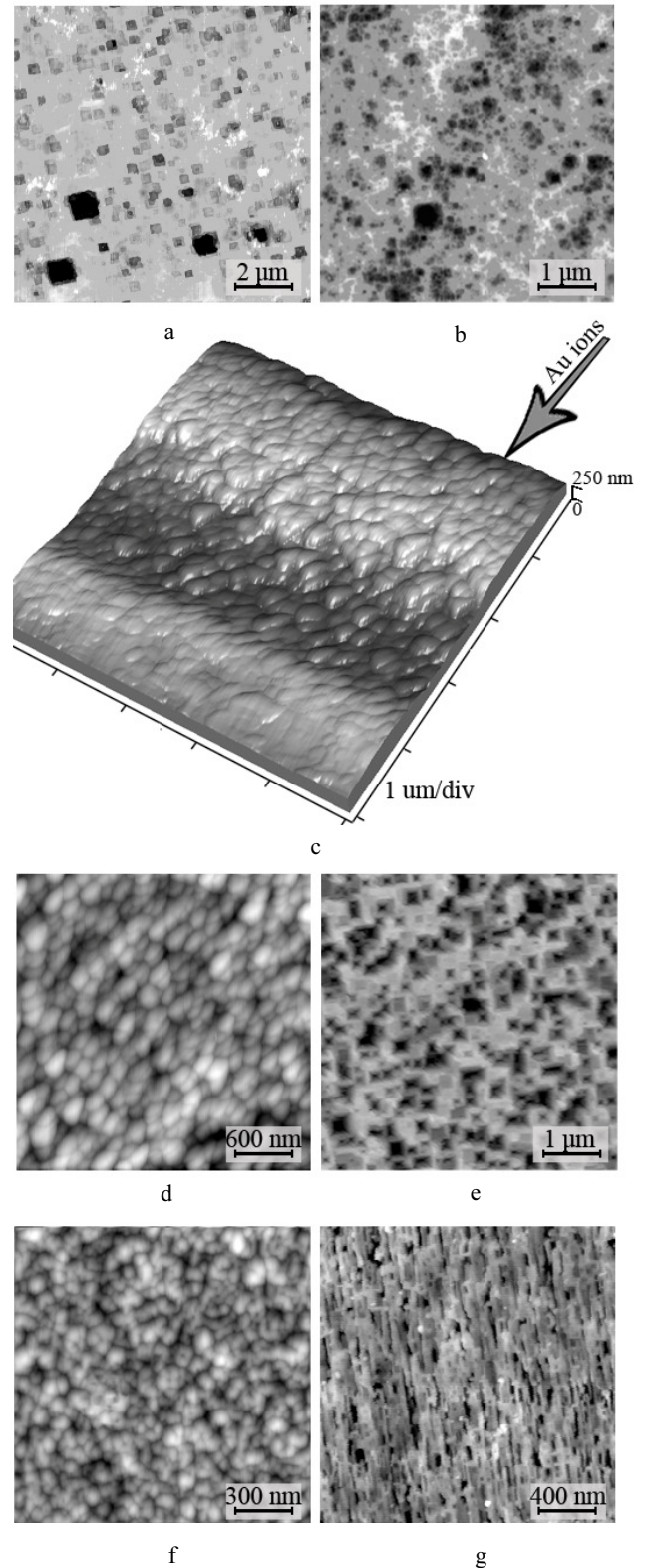


Fig. 1. AFM images of the irradiated LiF surface (after chemical etching): a – 3 MeV, 10^{12} Au/cm². The dark large etch pits denote the grown-in dislocations; b – 3 MeV, 10^{13} Au/cm²; c – 15 MeV, 5×10^{13} Au/cm² (3D view of the sample's cross-section); d – 15 MeV, 5×10^{13} Au/cm²; e – the same sample, after annealing at 750 K for 10 min; f – 2187 MeV, 10^{12} Au/cm², g – 2187 MeV, 10^{12} Au/cm² (view of the sample's cross section)

The selective chemical etching of crystals irradiated with GeV Au ions, for which the energy loss surpasses a threshold of 10 keV/nm, reveals ion tracks [15]. As in the case of dislocations, etching of ion tracks results in etch pits of a pyramidal shape. The etchable tracks exhibit a complex structure: a narrow (few nm) core region, consisting of closely spaced small aggregates of radiation defects, and surrounding halo zone consisting mainly of single electron and hole centres [5].

The observation of ion-induced dislocations on the surface irradiated with GeV Au ions becomes impossible due to the background of etchable tracks. We performed the experiments on samples irradiated with lighter ions (Ni) for which the energy loss is known to be below the threshold for the track etching [15]. The results showed formation of ion-induced dislocations, which density at fluence of 10^{10} ions/cm² reached about 10^8 cm⁻². Obviously, similar or more intense formation of dislocations could be expected also for GeV Au ions.

The high-fluence irradiation of crystals with GeV Au ions resulted in the nanostructuring of irradiated layer (Fig. 1, f and g). The nanostructure consists of long columnar grains with the width of 50 nm–100 nm.

The thermal stability of nanostructures formed under irradiation with MeV and GeV Au ions was investigated. The annealing above 810 K was required for the full recovery of the structure and properties. In all cases the nanostructure was transformed into the dislocation-rich structure during the initial stage of annealing (Fig. 1, e). After annealing the orientation of dislocation etch pits and dislocation rosettes around imprints coincided with those for single crystals.

3.2. Ion-induced change of hardness and modulus

Nanoindentation tests showed a significant increase of the hardness of samples irradiated with MeV-energy ions (Fig. 2, a).

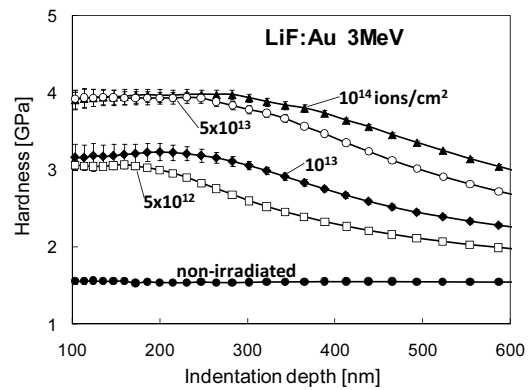
It should be taken into account that for a hard layer on a softer substrate the true hardness can be obtained in a limited indentation depth range. In order to exclude the effect of a softer bulk material, the indentation depth < 0.3 of the ion range for a given hardness ratio of irradiated layer and virgin bulk material is recommended [16]. Such condition is fulfilled in the plateau region of the hardness-indentation depth curves (Fig. 2).

The hardness solely depends on the applied fluence. The effect of hardening is observed above the threshold fluence of 5×10^{11} ions/cm². The hardness increases with fluence and above 10^{14} ions/cm² bends towards saturation at about 4.5 GPa, which exceeds the hardness of a virgin crystal by a factor of three. A further increase of hardness is limited due to transition of plastic deformation mechanisms from the dislocation related to those characteristic to nanostructured materials, which are facilitated by grain boundaries and a free volume.

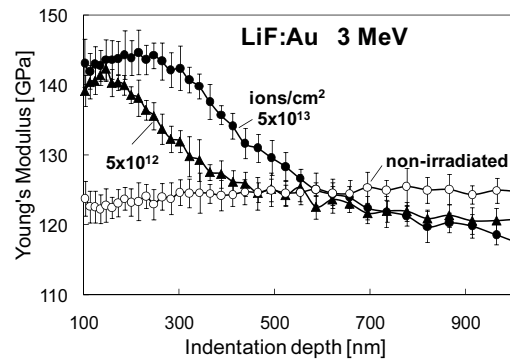
The corresponding ion-induced change of Young's modulus is comparatively small ($\sim 15\%$) (Fig. 2, b) and lies in the typical range for stress-induced variations of modulus. Moreover, the sign of the effect changes from a positive on the irradiated surface to a negative in deeper layers thus following the change of ion-induced long-range

stresses from compressive on the surface to tensile at the vicinity of interface between the irradiated layer and non-irradiated crystal [8].

The hardness data for all applied ion energies settle on a common curve (Fig. 3) thus indicating that the ion-induced hardening is nearly independent of ion energy. Obviously, such behavior emerges from the fact that the local deposited energy (E_{ion}/R) in the investigated range of MeV-ion energies is almost constant (Table 1). However, the increase of ion energy leads to the increased thickness of hardened layer as it is evident from the increase of the plateau region of the corresponding hardness-indentation depth curves (Fig. 4). The variation of the thickness of hardened layer with the ion energy is related to the change of ion range.



a



b

Fig. 2. Hardness (a) and Young's modulus (b) on the irradiated surface as a function of indentation depth for samples irradiated with 3 MeV Au ions at different fluences

To compare effects produced by MeV and GeV ions, a series of nanoindentation tests were conducted on LiF samples irradiated with 2187-MeV Au ions. The investigations were performed at the fluences ($2 \times 10^{11} - 10^{12}$) ions/cm². The results showed ion-induced hardening at fluences above the threshold of 5×10^9 ions/cm² at which the tracks of swift heavy ions start to overlap [9]. The hardness increases with fluence and at 10^{12} ions/cm² reaches about 3.9 GPa (Fig. 5). To achieve the same hardening by MeV ions, a higher fluence is required; however, the absorbed energy in comparison to GeV ions is lower. The irradiation at an ion beam current density of 100 nA/cm² corresponds to the flux of 3.12×10^{11} ions cm⁻² s⁻¹ for 3- and 5-MeV,

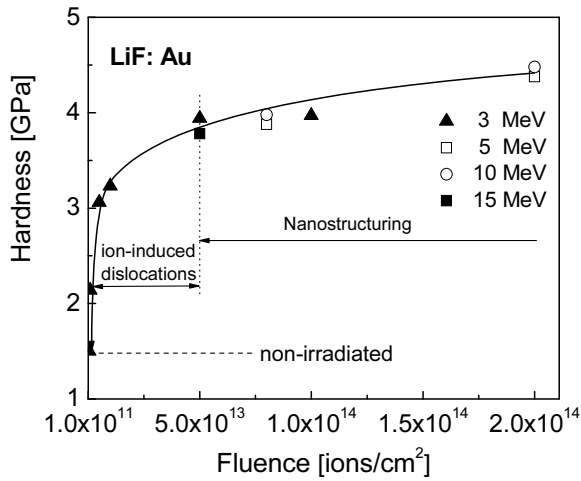


Fig. 3. Hardness as a function of fluence for different ion energies. The irradiations are performed at an ion beam current density of 100 nA/cm²

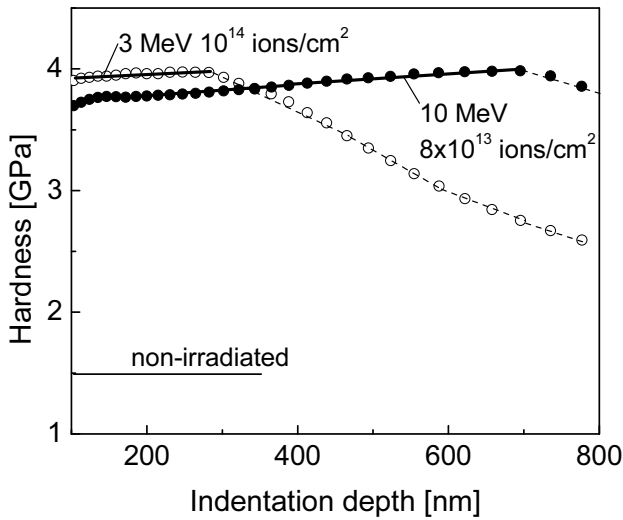


Fig. 4. Surface hardness as a function of indentation depth for samples irradiated with 3 MeV and 10 MeV Au ions under a comparable fluence. Solid curves denote the depth region where true hardness of the irradiated layer (not affected by a softer bulk material) is obtained

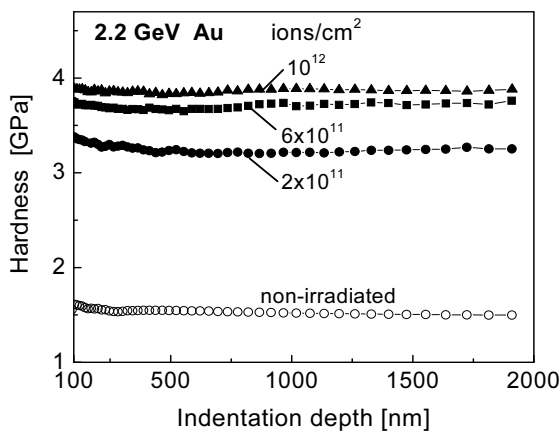


Fig. 5. Surface hardness as a function of indentation depth for samples irradiated with 2187 MeV Au ions at different fluences

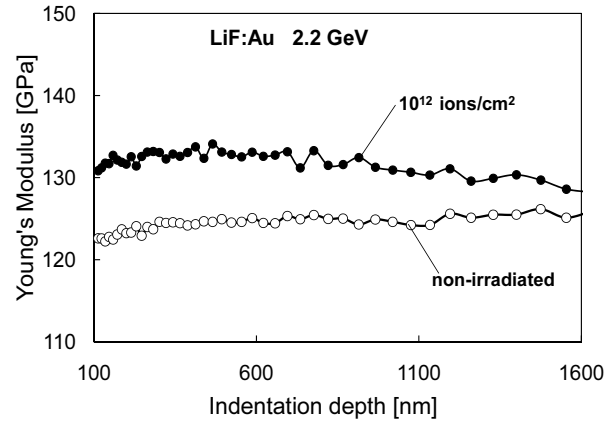


Fig. 6. Young's modulus as a function of indentation depth for samples irradiated with 2187 MeV Au ions at 10¹² ions/cm²

1.56×10¹¹ ions cm⁻² s⁻¹ for 10 MeV, and 10¹¹ ions cm⁻² s⁻¹ for 15-MeV Au ions. The flux for 2187-GeV Au ions was $\varphi \approx 10^8$ ions cm⁻² s⁻¹. The absorbed ion energy $E_{\text{ion}} \times \Phi$ for 2187-GeV Au ions ($\Phi = 10^{12}$ ions/cm²) is 2.2×10²¹ eV/cm² and for 3 MeV Au ions ($\Phi = 10^{14}$ ions/cm²) is 3×10²⁰ eV/cm².

The nanoindentation tests on the surface irradiated with GeV Au ions show the increase of modulus by about 12 % (Fig. 6). We relate this effect to long-range compressive stresses generated in the irradiated layer due to swelling processes.

4. DISCUSSION

The damage produced in LiF by Au ions with energy in the GeV range is localized in ion tracks, which have a complex structure: the core region possessing a radius of 1 nm–2 nm and consisting of small closely spaced aggregates of radiation defects, and surrounding halo region possessing a radius of 15 nm–30 nm and consisting of point defects, such as *F* centres [5]. More complex structure is formed at the stage of track overlapping when ions penetrate into the pre-irradiated areas. Under such conditions the saturation and aggregation of single defects is known to occur. The formation of complex color centres, fluorine bubbles and other products of radiolysis is detected by optical absorption spectroscopy and other methods [1–5, 17]. Similar aggregation processes are observed under irradiation with MeV-energy ions. However, the MeV ions produce higher volume concentration of color centres than the GeV-energy ions with the same absorbed energy. [11–13].

Structural modifications of LiF under irradiation with swift ions are of a special interest. In contrast to many insulators LiF does not amorphize even under a high dose of irradiations. This property is characteristic for materials with a strong ionic bonding. An irradiation with swift ions at moderate fluences typically leads to the formation of a composite-like structure in which the linear ion tracks and nanometre-sized precipitates and other aggregates of radiation defects are embedded in the crystalline LiF matrix.

The nanostructuring processes in the irradiated LiF are not studied in detail. The research is concerned mainly

with modifications of the surface topography, including the ion-induced formation of surface hillocks and figures of ion sputtering [18, 19]. Information about fragmentation processes in the bulk of irradiated crystals is limited. The reduction of the grain size in polycrystalline LiF films exposed to irradiation with MeV-energy Au ions is reported [20].

The present study shows that the high-fluence irradiation of LiF single crystals with MeV- and GeV- Au ions leads to the formation of bulk nanostructure consisting of grains with nanoscale dimensions. The structural study demonstrates the formation of ion-induced dislocations just before the stage of nanostructuring. It is well established that dislocation loops of vacancy and interstitial types are formed in LiF crystals by aggregation of single defects under different kinds of high-dose irradiation [21]. Another source of dislocations is ion-induced long-range mechanical stresses, which in irradiated samples can reach a critical value [8]. Accumulation of dislocations leads to fragmentation and nanostructuring via formation of dislocation networks and their transformation to grain boundaries. The grain boundaries and dislocations serve as sinks for mobile radiation defects and seeds for nucleation and growth of defect aggregates thus affecting the aggregation and annihilation processes of single defects. On the other hand, the segregation of defects and growth of the defect agglomerates on dislocations facilitate their immobilization.

The observed structural modifications strongly affect the strength properties of irradiated LiF. Remarkable ion-induced increase of the nanohardness as a structure-sensitive characteristic is found to occur. The deformation at the nanoindentation test develops under a high local stress and produced dislocations are moving at a high velocity (up to 10^5 cm/s [22]) that allows surmounting point defects, single colour centres and other comparatively weak obstacles. As a result, single defects play a minor role in the ion-induced hardening. However, the weak obstacles can reduce the mobility of dislocations moving at low velocity as it is observed in measurements of the arm length of dislocation rosettes around indents [9, 23].

The hardness is sensitive mainly to closely spaced aggregates of radiation defects, dislocations and grain boundaries. According to the additivity rule, the resulting hardening is a superposition of different strengthening phenomena.

The defect aggregates as strong obstacles for dislocations can alter the hardness mainly by the dispersion strengthening mechanism. Brief estimates performed using the Orowan's model [24] show that detectable increase of the hardness is expected at the average obstacle spacing $\lambda < 130$ nm. Such conditions can be reached at high-fluence irradiations at the stage of track overlapping.

According to the Taylor's model, the increase of flow stress (or hardness) scales with the dislocation density (ρ) as $\Delta\tau \sim \sqrt{\rho}$ [24]. Remarkable strengthening is expected at dislocation densities above 10^7 cm⁻²– 10^8 cm⁻². This limit is surpassed in irradiation experiments presented here.

The nanostructuring of LiF under the irradiation creates a large volume fraction of grain boundaries. Grain boundaries

serve as obstacles for dislocations and have a significant impact on the strength and hardness. For many materials the hardness (H) varies with grain size as $H \sim d^{-1/2}$ [25], where d is the average grain size. However, the result presented in Fig. 3 shows that a significant part of ion-induced hardening is reached before the stage of nanostructuring and confirms a strong contribution of dispersion strengthening and dislocation strengthening mechanisms. It should be taken into account that the hardness of irradiated LiF crystals saturates at about 4 GPa–4.5 GPa due to the change in mechanisms of plastic deformation.

5. CONCLUSIONS

The present study shows that the high-fluence irradiation of LiF single crystals with MeV and GeV Au ions leads to the formation of bulk nanostructures consisting of grains with nanoscale dimensions. The nanoindentation tests demonstrate a strong ion induced hardening, which is ascribed to dislocation impeding by assemblies of defect aggregates, such as H -centre and vacancy clusters, dislocation loops of vacancy and interstitial types, and grain boundaries.

Irradiation with ions in the MeV-energy range, which deposit a significant fraction of their energy via elastic collisions with the target atoms (nuclear energy loss), shows some peculiarities relative to GeV ions. About two orders of magnitude higher threshold fluence for hardening is observed in the case of MeV ions. However, the ratio of concentrations of complex F_n to single F centres in LiF crystals irradiated with 3 MeV–15 MeV Au ions is higher than in the case of GeV Au ions with a similar absorbed energy. This explains the higher localization of damage and higher changes in mechanical properties under the MeV-ion irradiation.

Acknowledgments

This research was partly supported by the Latvian Government grant No.09.1548.

M. Sorokin greatly acknowledges support from the Russian Foundation for the Basic Research (Grants 08-08-00603 and 09-08-12196).

The authors thank R. Papaleo for the irradiations with MeV ions.

REFERENCES

1. **Itoh, N., Stoneham, A. M.** Materials Modification by Electronic Excitations *Radiation Effects and Defects in Solids* 155 (1–4) 2001: pp. 277–290.
2. **Schwartz, K., Trautmann, C., El-Said, A. S., Neumann, R., Toulemonde, M., Knolle, W.** Color-center Creation in LiF under Irradiation with Swift Heavy Ions: Dependence on Energy Loss and Fluence *Physical Review B* 70 2004: pp. 1841041–1841048.
3. **Bonanza, E., Buford, S., Cassimere, A., Coryphée, E., Portion, L., Gradin, J. P., Donovan, J. L., Margery, J.** Defect Creation in Alkali-halides under Dense Electronic Excitations: Experimental Results *Nuclear Instruments and Methods in Physics Research B* 91 1994: pp. 134–139.
4. **Toulemonde, M., Boffard, S., Studer, F.** Swift Heavy Ions in Insulating and Conducting Oxides: Tracks and Physical

- Properties *Nuclear Instruments and Methods in Physics Research B* 91 1994: pp. 108–123.
5. **Schwartz, K., Trautmann, C., Steckenreiter, T., Geiß, O., Kramer, M.** Damage and Track Morphology in LiF Crystals Irradiated with GeV Ions *Physical Review B* 58 1998: pp. 11232–11240.
 6. **Regel, L. L., Regel, V. R., Boriskin, S. E., Knab, G. G., Urusovskaya, A. A., Alekseeva, L. I., Klechkovskaya, V. V.** Influence of Irradiation with Heavy Ions on the Defect Structure and Mechanical Properties of LiF Crystals *Physica Status Solidi (a)* 73 1982: pp. 255–256.
 7. **Kikuchi, A., Naramoto, H., Ozawa, K., Kazumata, Y.** Damage Profiles in Alkali Halides Irradiated with High-energy Heavy Ions *Nuclear Instruments and Methods in Physics Research B* 39 1989: pp. 724–727.
 8. **Manika, I., Maniks, J., Schwartz, K., Toulemonde, M., Trautmann, C.** Hardening and Long-range Stress Formation in Lithium Fluoride Induced by Energetic Ions *Nuclear Instruments and Methods in Physics Research B* 209 2003: pp. 93–97.
 9. **Manika, I., Maniks, J., Schwartz, K.** Swift-ion-induced Hardening and Reduction of Dislocation Mobility in LiF Crystals *Journal of Physics D: Applied Physics* 41 2008: pp. 074011–074015.
 10. **Manika, I., Maniks, J.** Ion-induced Hardening in LiF: Energy Loss and Fluence Effects *Nuclear Instruments and Methods in Physics Research B* 245 2006: pp. 260–263.
 11. **Schwartz, K., Sorokin, M. V., Lushchik, A., Lushchik, Ch., Vasil'chenko, E., Papaleo, R. M., de Souza, D., Volkov, A. E., Voss, K.-O., Neumann, R., Trautmann, C.** Color Center Creation in LiF Crystals Irradiated with 5- and 10-MeV Au Ions *Nuclear Instruments and Methods in Physics Research B* 266 1998: pp. 2736–2740.
 12. **Lushchik, A., Lushchik, Ch., Schwartz, K., Vasil'chenko, E., Papaleo, R., Sorokin, M., Volkov, A. E., Neumann, R., Trautmann, C.** Creation of Nanosize Defects in LiF Crystals under 5- and 10-MeV Au Ion Irradiation at Room Temperature *Physical Review B* 76 2007: pp. 0541141–05411411.
 13. **Sorokin, M. V., Papaleo, R. M., Schwartz, K.** Elastic Atomic Displacements and Color Center Creation in LiF Crystals Irradiated with 3-, 9- and 12-MeV Au Ions *Applied Physics A* 97 2009: pp. 143–146.
 14. **Ziegler, J. F., Biersack, P., Littmark, U.** The Stopping and Range of Ions in Matter. New York, Pergamon Press, 1985, SRIM - version 2010.01.
 15. **Trautmann, C., Schwartz, K., Geiss, O.** Chemical Etching of Ion Tracks in LiF Crystals *Journal of Applied Physics* 83 (7) 1998: pp. 3560–3564.
 16. **Manika, I., Maniks, J.** Effect of Substrate Hardness and Film Structure on Indentation Depth Criteria for Film Hardness Testing *Journal of Physics D: Applied Physics* 41 2008: pp. 0740081–0740086.
 17. **Davidson, A. T., Schwartz, K., Comins, J. D., Kozakiewicz, E. G., Toulemonde, M., Trautmann, C.** Vacuum Ultraviolet Absorption and Ion Track Effects in LiF Crystals Irradiated with Swift Ions *Physical Review B* 66 2002: pp. 2141021–2141028.
 18. **Müller, A., Neumann, R., Schwartz, K., Trautmann, C.** Heavy-ion Induced Modification of Lithium Fluoride Observed by Scanning Force Microscopy *Applied Physics A* 66 1998: pp. S1147–S1150.
 19. **Gebeshuber, I. C., Cernusca, S., Aumayr, F., Winter, H. P.** AFM Search for Slow MCI-produced Nanodefects on Atomically Clean Monocrystalline Insulator Surfaces *Nuclear Instruments and Methods in Physics Research B* 205 2003: pp. 751–757.
 20. **Kumar, M., Singh, F., Khan, S. A., Tripathi, A., Avasthi, D. K., Pandey, A. C.** Swift Heavy Ion Induced Structural and Optical Modifications in LiF Thin Film *Journal of Physics D: Applied Physics* 38 2005: pp. 637–641.
 21. **Kawamata, Y.** The Formation of Dislocation Loops and the Outgrows of Crystallites by Electron Irradiation of the Alkali Halide Foils *Journal de Physique* 12 1976: pp. C502–C507.
 22. **Johnston, W. G., Gilman, J. J.** Dislocation Velocities, Dislocation Densities and Plastic Flow in LiF Crystals *Journal of Applied Physics* 30 1959: pp. 129–141.
 23. **Berzina, I. G., Berman, I. B.** Dislocation Mobility in Irradiated Crystals *Kristallographia* 9 1964: pp. 260–264 (in Russian).
 24. **Kelly, A., Nicholson, R. B.** Precipitation Hardening. Ed. B. Chalmers, New York, Pergamon Press, 1963: 391 p.
 25. Grain Boundaries and Interfaces. Eds. **Chaudhari, P., Matthews, J. W.** Amsterdam, North-Holland, 1972: 630 p.